Optimal Decentralized Protocols for Electric Vehicle Charging

Lingwen Gan Ufuk Topcu Steven Low

***Abstract*—We propose decentralized algorithms for optimally scheduling electric vehicle (EV) charging. The algorithms exploit the elasticity and controllability of electric vehicle loads in order to fill the valleys in electric demand profiles. We first formulate a global optimization problem, whose objective is to impose a generalized notion of valley-filling, and study the properties of optimal charging profiles. We then give two decentralized algorithms, one synchronous (i.e., information update takes place in each iteration) and one asynchronous (i.e., EVs may use outdated information with bounded delay in some of the iterations) to solve the problem. In each iteration of the proposed algorithms, EVs choose their own charging profiles according to the price profile broadcast by the utility, and the utility updates the price profile to guide their behavior. Both algorithms are guaranteed to converge to optimal charging profiles (that are as "flat" as they can possibly be) irrespective of the specifications (e.g., maximum charging rate and deadline) of electric vehicles. Furthermore, both algorithms only require each EV solving its local problem, hence their implementation requires low computation capability. We also extend the algorithms to accommodate the objective of tracking a given demand profile and to real-time implementations.**

***Index Terms*—Distributed optimal control; electrical vehicle charging; controllable electric loads.**

NOTATION

t	time index, $t \in \mathcal{T} := \{1, \ldots, T\}$
n	index of electric vehicles (EVs), $n \in \mathcal{N} := \{1, \ldots, N\}$
D	base demand profile
r_n	charging profile of EV n
r	charging profile of all EVs
R_r	aggregated charging profile corresponding to r
$\overline{r}_n$	charging rate upper bound for EV n
R_n	charging rate sum of EV n
$\mathcal{F}_n$	set of feasible charging profiles for EV n
$\mathcal{F}$	set of feasible charging profiles for all EVs
$\mathcal{O}$	set of optimal charging profiles
p	price profile
$\preceq$	if $a, b \in \mathbb{R}^n$, $a \preceq b \Leftrightarrow a_i \leq b_i$ for all $i \in \{1, \ldots, n\}$
$\succeq$	if $a, b \in \mathbb{R}^n$, $a \succeq b \Leftrightarrow a_i \geq b_i$ for all $i \in \{1, \ldots, n\}$
x^+	$\max\{0, x\}$
$\langle x, y \rangle$	for $x, y \in \mathbb{R}^n$, $\langle x, y \rangle := \sum_{k=1}^{n} x_k y_k$
$\|x\|$	for $x \in \mathbb{R}^n$, $\|x\| := \sqrt{\langle x, x \rangle}$

I. INTRODUCTION

Electric vehicles (EVs) offer significant potential for increasing energy efficiency in transportation, reducing greenhouse gas emissions, and relieving reliance on foreign oil [1]. Currently, several types of EVs are either already in the U.S. market or about to enter [2], and electrification of transportation is at the forefront of many research and development agendas [3]. On the other hand, the potential comes with a multitude of challenges including those in the integration into the electric power grid. EV charging increases the electricity demand, and potentially amplifies the peak demand or creates new peaks [4]. EV charging also increases the demand side uncertainties, and presumably reduces the distribution circuit (e.g., transformer) lifespan [5]. Moreover, power losses and voltage deviations become more likely [6].

The simulation-based study in [7] suggests that, if no regulation on EV charging is implemented, even a 10% penetration of EVs may cause unacceptable voltage deviations. On the other hand, many studies demonstrate that adopting "smart" charging strategies can mitigate some of the integration challenges, defer infrastructure investment needed otherwise, and even help stabilize the grid. For example, scheduling EV charging so that the aggregated EV load fills the overnight valley in electricity demand may reduce daily cycling of power plants and operational costs that come along. Furthermore, the energy stored in EVs may be utilized as an alternative ancillary service resource [8] for regulating the voltage in distribution circuit, ride-through support for fault protection, and even compensating fluctuating renewable energy generation [9].

Studies on EV charging control roughly fall into three categories: effect of time-of-use prices [10], centralized charging scheduling [6], [9], [11], and decentralized charging scheduling [12] [13]. Reference [10] explores the effect of higher price during peak hours on shifting EV load, but does not provide strategies for setting the price. Reference [6], [9], [11] study centralized control strategies that minimize power losses and load variance, or maximize load factor and supportable EV penetration level. These strategies require a centralized structure to collect information from all the EVs and centrally optimize over their charging profiles. The size of this centralized optimization increases with the increasing number of EVs. Hence, a decentralized coordination scheme is potentially more suitable for the case with a high penetration level of EVs.

Decentralized coordination — potentially enabled by technologies such as energy management systems, home area networks, and controlled charging units for EVs — has attracted recent attention. Reference [12] demonstrates, through a simulation-based study, that total demand profile can be flattened by introducing load-side participation into the power market. They propose a decentralized strategy, but do not provide any analytical optimality guarantees. Reference [13]

The authors are with Engineering and Applied Sciences at the California Institute of Technology, e-mail: lgan@caltech.edu; utopcu@cds.caltech.edu; slow@caltech.edu.

proposes another decentralized charging strategy, with proved optimality in the case where all EVs plug in for charging at the same time with the same deadline, and need to consume the same amount of energy at the same maximum charging rate. For future reference, we call this setting *homogeneous*.

The contributions of the current paper include the following. First, we define optimal charging profiles of EVs explicitly (this definition generalizes the implicit definition in [13]). Second, we propose a decentralized charging strategy that guarantees optimality in both homogeneous and non-homogeneous cases, where EVs can plug in at different times with different deadlines, and consume different amount of energy at different maximum charging rate. Third, we remove the artificial tracking error penalty in EV owners' objective in [13] by introducing another penalty term that vanishes at convergence. Fourth, we modify the decentralized algorithm to accommodate asynchronous computations, i.e., EVs may make their decisions at different times with potentially outdated information. We prove that the modified asynchronous algorithm preserves guaranteed optimality. Finally, we extend the algorithms to track a given demand profile and to real-time implementation.

The rest of the paper is organized as follows. Section II formulates the EV charging protocol design problem as a finite-horizon optimal control problem. Section III explores properties of optimal charging profiles of this optimal control problem. Section IV is dedicated to the presentation of two decentralized optimization algorithms for solving the optimal control problem and their convergence proofs. Numerical case studies are presented in section V, and potential extensions of the proposed work are summarized in section VI.

II. Problem Formulation

Consider a scenario where an electric utility negotiates with N electric vehicles (EVs) over T time slots of length ΔT on their charging profiles. The utility is assumed to know (precisely predict) the inelastic base demand profile (aggregated non-EV demand) and aims to shape the aggregated charging profile of EVs to flatten the total demand (base demand plus EV demand) profile. Each EV can charge after it plugs in and needs to be charged a specified amount of electricity by its deadline. For instance, an EV may plug in for charging at 9:00pm, specifying that it needs to be fully charged by 6:00am next morning, or reach at least 80% state of charge (SOC) by 4:00am next morning. In each time slot, the charging rate of an EV is a constant. Let $D(t)$ denote the base load in slot t, $r_n(t)$ denote the charging rate of EV n in slot t, $r_n := (r_n(1), \ldots, r_n(T))$ denote the charging profile of EV n, for $n \in \mathcal{N} := \{1, \ldots, N\}$ and $t \in \mathcal{T} := \{1, \ldots, T\}$. The term "negotiate" will be clear in section IV, where decentralized algorithms for solving the finite-horizon optimal control problem formulated in this section are presented. Roughly speaking, this optimal control problem formalizes the intent of flattening the total demand profile, which is captured by the objective function

$$L(r) = L(r_1, \ldots, r_N) := \sum_{t=1}^{T} U\left(D(t) + \sum_{n=1}^{N} r_n(t)\right). \quad (1)$$

In (1) and hereafter, $r := (r_1, \ldots, r_N)$ denotes a charging profile of all EVs. The map $U : \mathbb{R} \to \mathbb{R}$ is strictly convex.

The charging profile r_n of EV n is considered to take values in the interval $[0, \overline{r}_n]$ for some given $\overline{r}_n \succeq 0$.[1] In order to impose arrival time and deadline constraints, $\overline{r}_n$ is considered to be time-dependent with $\overline{r}_n(t) = 0$ for slots t before the arrival time and after the deadline of EV n. Hence

$$0 \le r_n(t) \le \overline{r}_n(t), \ n \in \mathcal{N}, \ t \in \mathcal{T}. \quad (2)$$

For EV $n \in \mathcal{N}$, let B_n, $s_n(0)$, $s_n(T)$ and η_n denote its battery capacity, initial state of charge, final state of charge and charging efficiency. The constraint that EV n needs to reach $s_n(T)$ state of charge by its deadline is captured by the total energy stored over time horizon

$$\eta_n \sum_{t \in \mathcal{T}} r_n(t) \Delta T = B_n(s_n(T) - s_n(0)), \ n \in \mathcal{N}. \quad (3)$$

Define the charging rate sum

$$R_n := B_n(s_n(T) - s_n(0))/(\eta_n \Delta T)$$

for $n \in \mathcal{N}$. Then, the constraint in (3) can be written as

$$\sum_{t=1}^{T} r_n(t) = R_n, \ n \in \mathcal{N}. \quad (4)$$

For instance, if an EV plugs in with $s_n(0) = 10\%$ and needs to reach $s_n(T) = 80\%$ by its deadline, assuming that charging efficiency is $\eta_n = 0.7$, its battery capacity is $B_n = 10$kWh, and each time slot is 15 minutes, then

$$R_n = \frac{10kWh \times (0.8 - 0.1)}{0.7 \times 15minutes} = 40kW.$$

Reference [15] summarizes some of the recently announced EV models. Typical values of $\overline{r}_n$ and R_n can be derived for these models (and used in the numerical case studies in section V).

Definition 1: Let $U : \mathbb{R} \to \mathbb{R}$ be strictly convex. A charging profile $r = (r_1, \ldots, r_N)$ is

1) *feasible*, if it satisfies the constraints (2) and (4);
2) *optimal*, if it solves the optimal charging (OC) problem

$$\textbf{OC} \begin{cases} \underset{r_1,\ldots,r_N}{\text{minimize}} & \sum_{t=1}^{T} U\left(D(t) + \sum_{n=1}^{N} r_n(t)\right) \\ \text{subject to} & 0 \le r_n(t) \le \overline{r}_n(t), \ t \in \mathcal{T}, n \in \mathcal{N}; \\ & \sum_{t=1}^{T} r_n(t) = R_n, \ n \in \mathcal{N}; \end{cases} \quad (5)$$

3) *valley-filling*, if there exists $A \in \mathbb{R}$ such that

$$\sum_{n \in \mathcal{N}} r_n(t) = [A - D(t)]^+, \ t \in \mathcal{T}.$$

[1] Each EV $n \in \mathcal{N}$ can charge after it plugs in at $plug_n$ and before its deadline $dead_n$. Hence, $r_n(t) = 0$ for $t \notin [plug_n, dead_n]$. During $t \in [plug_n, dead_n]$, the EV can charge at some fixed charging rate level, which we denote by r_n^{max}. For instance, $r_n^{max} = 1.4$kW if EV n uses single-phase, Level I charging, and $r_n^{max} = 3.3$kW if EV n uses single-phase, Level II charging [15]. The discreteness in charging rate makes the problem difficult to solve, so we assume that the EV can charge at any rate between 0 and r_n^{max}. Hence, if we define a time varying upper bound

$$\overline{r}_n(t) = \begin{cases} 0 & \text{if } t < plug_n \text{ or } t > dead_n \\ r_n^{max} & \text{if } plug_n \le t \le dead_n \end{cases},$$

then the charging rate constraint can be summarized by (2).

Remark 1: Optimality of a charging profile r is independent of the choice of the utility function U (proved in Theorem 2). That is, if r is optimal with respect to a strictly convex utility function, then it is optimal with respect to any other strictly convex utility function. Therefore, we can choose $U(x) = x^2$ without loss of generality, and see that optimal charging profiles minimize the l_2 norm of the total demand profile. Since the l_1 norm is a constant for all feasible r due to (4), minimizing the l_2 norm "flattens" the total demand profile.

Remark 2: If the objective is to track a given demand profile G rather than to flatten the total demand, the objective function can be modified as

$$\sum_{t=1}^{T} U\left(D(t) + \sum_{n=1}^{N} r_n(t) - G(t)\right). \tag{6}$$

For notational convenience, we focus on the objective function in (1), and briefly discuss this extension in section VI-A.

III. Optimal Charging Profile

In this section, we investigate the properties of optimal charging profiles. For notational simplicity, for a given charging profile $r = (r_1, \ldots, r_N)$, let

$$R_r := \sum_{n \in \mathcal{N}} r_n$$

denote its corresponding aggregated charging profile.

Property 1: If a feasible charging profile r is valley-filling, then it is optimal.

Proof: For any feasible and valley-filling r, its corresponding aggregated charging profile R_r is the unique solution to the following problem:

$$\begin{aligned} \underset{R}{\text{minimize}} \quad & \textstyle\sum_{t\in\mathcal{T}} U\left(D(t) + R(t)\right) \\ \text{subject to} \quad & \textstyle\sum_{t\in\mathcal{T}} R(t) = \sum_{n\in\mathcal{N}} R_n, \\ & R \succeq 0. \end{aligned} \tag{7}$$

For any r' feasible for problem OC, $R_{r'}$ is feasible for (7). Furthermore, the objective function in (7) evaluated at $R_{r'}$ is equal to $L(r')$. Hence, the optimal value d_* of (7) is a lower bound for the optimal value p_* of problem OC. The aggregated profile R_r attains d_*, so $L(r) = d_* \leq p_*$. Since r is feasible for problem OC, $L(r) \geq p^*$. Hence, $L(r) = p^*$, and r is optimal for problem OC. ■

Define $\mathcal{F}_n := \left\{r_n |\ 0 \preceq r_n \preceq \overline{r}_n, \sum_{t\in\mathcal{T}} r_n(t) = R_n\right\}$ as the set of feasible charging profiles for EV n. Then,

$$\mathcal{F} := \mathcal{F}_1 \times \cdots \times \mathcal{F}_N$$

is the set of feasible charging profiles $r = (r_1, \ldots, r_N)$.

Property 2: If $\mathcal{F}$ is non-empty, optimal charging profiles exist.

Proof: Since $\mathcal{F}_n$ is compact, $\mathcal{F}$ is also compact. Since L is continuous, its minimum value is attained at some $r \in \mathcal{F}$, which is an optimal charging profile. ■

Valley-filling is our intuitive notion of optimality. However, it may not be always achievable. For example, the "valley" in inelastic base demand may be so deep that even if all EVs charge at their maximum rate, it is still not completely filled, e.g., at 4:00 in Figure 1 (bottom). Besides, EVs may have stringent deadlines such that the potential for shifting the load over time to yield valley-filling is limited. The notion of optimality in Definition 1 relaxes these restrictions as a result of Property 2. Moreover, it agrees with the intuitive notion of optimality when valley-filling is achievable as a result of Property 1, illustrated in Figure 1 (top). We now establish an equivalence relation between charging profiles, and show that optimal charging profiles form an equivalence class.

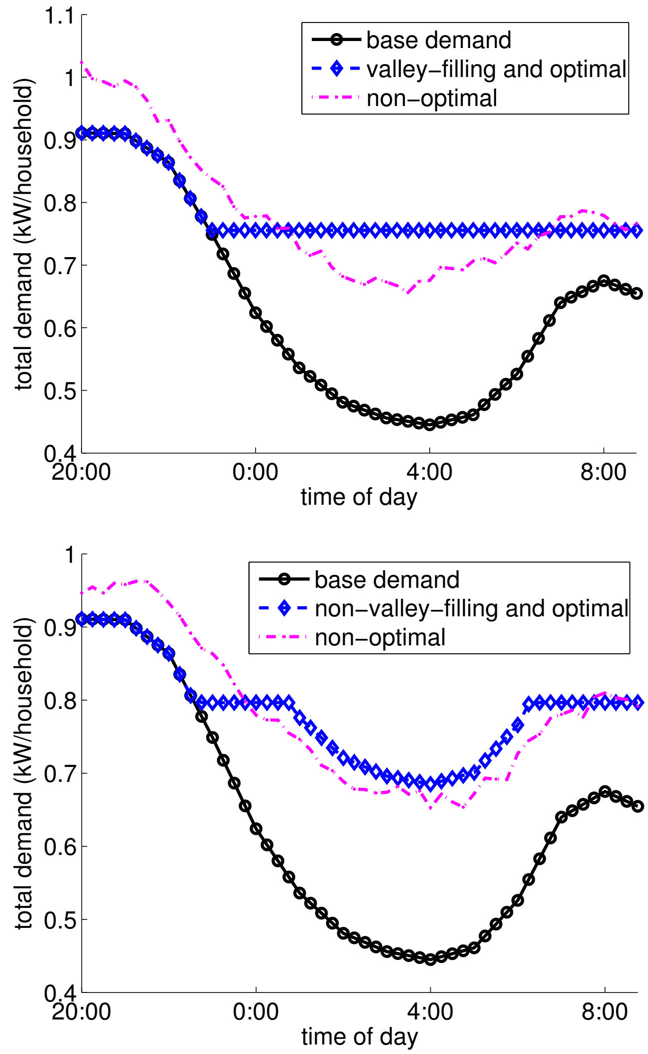

Fig. 1. Base demand profile is the average residential load in the service area of Southern California Edison (SCE) from 20:00 on 02/13/2011 to 9:00 on 02/14/2011 [16]. Optimal total demand profile curve corresponds to the outcome of Algorithm A1 (introduced in section IV) with $U(x) = x^2$. With different specifications for EVs (e.g., maximum charging rate r_n^{max}), optimal charging profile can be valley-filling (top figure) or non-valley-filling (bottom figure). A hypothetical non-optimal curve is shown in purple with dash-dot line.

Definition 2: Two feasible charging profiles r and r' are *equivalent*, provided that $R_r = R_{r'}$, i.e., r and r' have the same aggregated charging profile. We denote this relation by $r \sim r'$.

It is easy to check that the relation $\sim$ is an equivalence relation. Define equivalence classes $\{r' \in \mathcal{F} |\ r' \sim r\}$ with

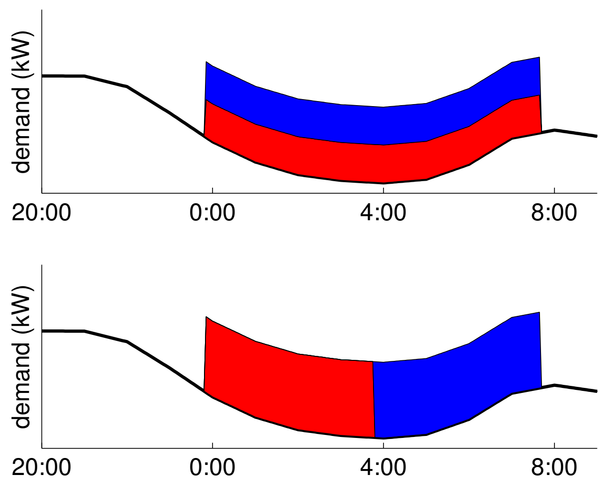

Fig. 2. An example of equivalent charging profiles. In both top and bottom figures, red region corresponds to the charging profile of one EV, while blue region corresponds to the charging profile of another EV. Since aggregated charging profiles in both figures equal, the charging profile r in the top figure is equivalent to the charging profile r' in the bottom figure.

representatives $r \in \mathcal{F}$, and

$$\mathcal{O} := \{r \in \mathcal{F} \mid r \text{ optimal}\}$$

as the set of optimal charging profiles.

Theorem 1: If $\mathcal{F}$ is non-empty, then $\mathcal{O}$ is non-empty, compact, convex, and an equivalence class of the relation $\sim$.

Proof: Property 2 implies that $\mathcal{O}$ is nonempty. Let r be an arbitrary charging profile in $\mathcal{O}$, and define equivalence class

$$\mathcal{O}' := \{r' \in \mathcal{F} \mid r' \sim r\}.$$

Then $\mathcal{O}'$ is closed and convex. Since $\mathcal{F}$ is compact, the set $\mathcal{O}'$, as a closed subset of $\mathcal{F}$, is also compact. Hence, $\mathcal{O}'$ is non-empty, compact, convex, and an equivalence class.

We are left to prove that $\mathcal{O} = \mathcal{O}'$. It is easy to see that $\mathcal{O}' \subseteq \mathcal{O}$, and we prove $\mathcal{O} \subseteq \mathcal{O}'$ as following. For any $r' \in \mathcal{O}$, it follows from the first order optimality condition for (5) that

$$\langle U'(D + R_r), R_{r'} - R_r\rangle \geq 0,$$
$$\langle U'(D + R_{r'}), R_r - R_{r'}\rangle \geq 0.$$

Adding the two inequalities up yields

$$\langle U'(D + R_r) - U'(D + R_{r'}), R_r - R_{r'}\rangle \leq 0.$$

However, since U' is strictly increasing, we have

$$\langle U'(D + R_r) - U'(D + R_{r'}), R_r - R_{r'}\rangle \geq 0,$$

and equality is obtained if and only if $R_r = R_{r'}$. Hence, we know that $R_r = R_{r'}$, $r' \sim r$, $r' \in \mathcal{O}'$, and $\mathcal{O} \subseteq \mathcal{O}'$, this completes the proof. ∎

Corollary 1: Optimal charging profile may not be unique.

Theorem 2: The set $\mathcal{O}$ of optimal charging profiles does not depend on the choice of U. That is, if r^* is optimal with respect to a strictly convex utility function, then r^* is also optimal with respect to any other strictly convex utility function.

Proof: Let $\hat{\mathcal{O}}$ denote the set of optimal charging profiles with respect to $\hat{U}(x) = x^2$, $\mathcal{O}_U$ denote the set of optimal charging profiles with respect to an arbitrary, strictly convex U. We only need to show that $\mathcal{O}_U = \hat{\mathcal{O}}$. According to Theorem 1, $\mathcal{O}_U$ is an equivalence class represented by some charging profile $r^* = (r_1^*, \ldots, r_N^*)$. Define $R^* := R_{r^*}$, then

$$\langle U'(D + R^*), r_n' - r_n^*\rangle \geq 0$$

for $n \in \mathcal{N}$ and $r_n' \in \mathcal{F}_n$ according to the optimality of r^* with respect to U. Hence, r_n^* minimizes $\langle U'(D + R^*), r_n\rangle$ over $r_n \in \mathcal{F}_n$. Since U' is strictly increasing and $\sum_{t=1}^{T} r_n(t)$ is a constant for $r_n \in \mathcal{F}_n$, r_n^* minimizes $\langle D + R^*, r_n\rangle$ over $r_n \in \mathcal{F}_n$, hence

$$\langle D + R^*, r_n' - r_n^*\rangle \geq 0$$

for $n \in \mathcal{N}$ and $r_n' \in \mathcal{F}_n$. Sum up over $n \in \mathcal{N}$ to obtain

$$\langle D + R_r, R_{r'} - R_r\rangle \geq 0$$

for all $r' \in \mathcal{F}$, which is the first order optimality condition for minimizing $L(r)$ with $U(x) = x^2$. Hence, $r^* \in \hat{\mathcal{O}}$, and it follows from Theorem 1 that $\mathcal{O}_U = \hat{\mathcal{O}}$. ∎

The optimal solution to problem OC provides a uniform means for defining optimality even when valley-filling is not achievable, and Theorem 2 implies that this optimality notion is intrinsic, independent of the choice of U.

IV. Decentralized Algorithms

In this section, we propose two decentralized algorithms, Algorithms A1 and A2 discussed below, for computing optimal charging profiles as the solution of the finite-horizon optimal control problem OC. By decentralized, we mean that EVs choose their own charging profiles, instead of being instructed by a centralized infrastructure. The utility only uses control signals, e.g. prices, to guide EVs' decisions. We assume that all EVs are available for negotiation at the beginning of the planning horizon (even though they are not necessarily available for charging as reflected by time-varying $\overline{r}_n$). Algorithm A1 is a synchronous algorithm requiring all EVs to make decisions at the same time with up-to-date information, while Algorithm A2 is asynchronous, allowing EVs to make decisions at different times using potentially outdated information with bounded delays in information update. We prove the convergence of both algorithms to optimal charging profiles under certain mild conditions.

A. Synchronous Decentralized Algorithm

We now present the basic decentralized algorithm and prove its convergence to optimal charging profiles. Figure 3 shows the information exchange between the utility and the EVs for the implementation of this algorithm. Given the "price" profile broadcast by the utility, each EV chooses its charging profile independently, and reports back to the utility. The utility guides their behavior by altering the "price" profile. We assume U' is Lipschitz with the Lipschitz constant $\beta > 0$, i.e.,

$$|U'(x) - U'(y)| \leq \beta|x - y|$$

for all x, y.

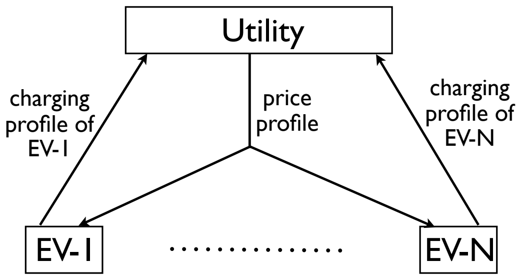

Fig. 3. Schematic view of the information flow patterns between the utility and the EVs. Given the "price" profile, the EVs choose their charging profiles independently. The utility guides their decisions by altering the "price" profile based on total demand profile.

Algorithm A1:
Given planning horizon $\mathcal{T}$, the maximum number K of iterations, error tolerance $\epsilon > 0$, base load profile D, the number N of EVs, charging rate sum R_n and charging rate upper bound $\overline{r}_n$ for EV $n \in \mathcal{N}$, pick a step size γ satisfying

$$0 < \gamma < \frac{1}{N\beta}.$$

1) Initialize the "price" profile and the charging profile as
$$p^0(t) := U'(D(t)),\ r_n^0(t) := 0$$
for $t \in \mathcal{T}$ and $n \in \mathcal{N}$, $k \leftarrow 0$.
2) The utility broadcasts γp^k to all EVs.
3) Each EV $n \in \mathcal{N}$ calculates a new charging profile r_n^{k+1} as the solution to the following optimization problem
$$\begin{aligned} \min_{r_n} \quad & \sum_{t\in\mathcal{T}} \gamma p^k(t) r_n(t) + \frac{1}{2}\left(r_n(t) - r_n^k(t)\right)^2 \quad (8)\\ \text{s.t.} \quad & 0 \le r_n(t) \le \overline{r}_n(t),\ t \in \mathcal{T};\\ & \sum_{t\in\mathcal{T}} r_n(t) = R_n, \end{aligned}$$
and reports r_n^{k+1} to the utility.
4) The utility collects charging profiles r_n^{k+1} from the EVs, and updates the "price" as
$$p^{k+1}(t) := U'\left(D(t) + \sum_{n=1}^{N} r_n^{k+1}(t)\right) \quad (9)$$
for $t \in \mathcal{T}$.
If $\left\|p^{k+1} - p^k\right\| \le \epsilon$, return $p^{k+1},\ r_n^{k+1}$ for all n.
5) If $k < K$, $k \leftarrow k+1$, and go to step (2).
Else, return $p^K,\ r_n^K$ for all n.

Remark 3: Algorithm A1 is suitable for decentralized implementation. That is, it necessitates both the EVs and the utility to use information locally available.

Remark 4: The "price" signal p is actually a control signal used by the utility to guide the EVs in choosing their charging profiles, and is not necessarily the real electricity price.

In each iteration, the algorithm can be split into two parts. In the first part, EV n updates its charging profile to minimize its objective function as (8). There are two terms in the objective: the first term is the "cost" and the second term penalizes deviations from the profile computed in the previous iteration. The extra penalty term ensures convergence of Algorithm A1, and vanishes as $k \to \infty$ (proved in Theorem 4). Hence, the objective function of each EV boils down to its "cost" as $k \to \infty$. Intuitively, the smaller γ is, the more significant the penalty term becomes, the less r_n^{k+1} is going to deviate from r_n^k, and the more likely Algorithm A1 will converge. When $\gamma < \frac{1}{N\beta}$, Algorithm A1 converges to optimal charging profiles (proved in Theorem 3). It can be seen that the upper bound $\overline{\gamma} := \frac{1}{N\beta}$ of γ is inversely proportional to the number N of EVs and the Lipschitz constant β of U'. For large N, each EV has to update its charging profile slower since the aggregated profile update is roughly N times amplified. Hence, the penalty term should be larger, and $\overline{\gamma}$ should be smaller. When the Lipschitz constant β is larger, the same difference in total demand is going to cause a larger difference in U', or p according to (9). Hence, for the two terms in (8) to remain the same scale, $\overline{\gamma}$ should decrease. In conclusion, the upper bound $\overline{\gamma} = \frac{1}{N\beta}$ agrees with our intuition. In the second part of the iteration, the utility updates the "price" profile according to (9). It sets higher prices for slots with higher total demand, to give EVs the incentive to shift their energy consumption to slots with lower total demand.

We now establish the convergence of Algorithm A1 to the set $\mathcal{O}$ of optimal charging profiles. Let the superscript k for each variable denote its respective value in iteration k. For example, r_n^k denotes the charging profile of EV n in iteration k. Similarly,

$$R^k := \sum_{n=1}^{N} r_n^k$$

denotes the aggregated charging profile in iteration k.

Lemma 1: If the set $\mathcal{F}$ of feasible charging profiles is non-empty, then the inequality

$$\langle \gamma p^k, r_n^{k+1} - r_n^k \rangle \le -\left\|r_n^{k+1} - r_n^k\right\|^2 \quad (10)$$

holds for $n \in \mathcal{N}$ and $k \ge 1$.

Proof: For $n \in \mathcal{N}$ and $k \ge 1$, it follows from the first order optimality condition for (8) that

$$\langle \gamma p^k + r_n^{k+1} - r_n^k, r_n - r_n^{k+1} \rangle \ge 0 \quad (11)$$

for all $r_n \in \mathcal{F}_n$. Since $r_n^k \in \mathcal{F}_n$,

$$\langle \gamma p^k + r_n^{k+1} - r_n^k, r_n^k - r_n^{k+1} \rangle \ge 0,$$

and (10) follows. ∎

Lemma 2: If $\mathcal{F}$ is non-empty, then for $n \in \mathcal{N}$ and $k \ge 1$, $r_n^{k+1} = r_n^k$ if and only if, for all $r_n \in \mathcal{F}_n$,

$$\langle p^k, r_n - r_n^k \rangle \ge 0. \quad (12)$$

Lemma 2 follows from (11) and strict convexity of (8). Recall that $\mathcal{O}$ denotes the set of optimal charging profiles.

Theorem 3: If $\mathcal{F}$ is non-empty, then $r^k \to \mathcal{O}$ as $k \to \infty$.

Proof: Define $D^k := D + R^k$. Then,

$$\begin{aligned} L(r^{k+1}) &= \sum_{t=1}^{T} U\left(D^{k+1}(t)\right) \\ \leq & \sum_{t=1}^{T} U\left(D^k(t)\right) - p^{k+1}(t)\left(R^k(t) - R^{k+1}(t)\right) \\ = & \; L(r^k) + \langle p^{k+1}, R^{k+1} - R^k \rangle \\ \leq & \; L(r^k) + \langle p^k + \beta\left(R^{k+1} - R^k\right), R^{k+1} - R^k \rangle \\ = & \; L(r^k) + \beta \left\| R^{k+1} - R^k \right\|^2 + \sum_{n=1}^{N} \langle p^k, r_n^{k+1} - r_n^k \rangle \\ \leq & \; L(r^k) + \beta \left\| R^{k+1} - R^k \right\|^2 - \frac{1}{\gamma} \sum_{n=1}^{N} \left\| r_n^{k+1} - r_n^k \right\|^2 \\ \leq & \; L(r^k) + \left(N\beta - \frac{1}{\gamma} \right) \sum_{n=1}^{N} \left\| r_n^{k+1} - r_n^k \right\|^2 \qquad (13) \\ \leq & \; L(r^k) \end{aligned}$$

for $k \geq 1$. The first inequality is due to convexity of U, the second inequality is due to the definition of the Lipschitz constant β, the third inequality is due to Lemma 1, and the fourth inequality is due to the Cauchy-Schwarz theorem. It is easy to check that $L(r^{k+1}) = L(r^k)$ if and only if $r^{k+1} = r^k$.

If $r^{k+1} = r^k$, then it follows from Lemma 2 that

$$\langle p^k, r_n' - r_n^k \rangle \geq 0$$

for all n and $r_n' \in \mathcal{F}_n$. Hence,

$$\langle p^k, R_{r'} - R^k \rangle = \sum_{n=1}^{N} \langle p^k, r_n' - r_n^k \rangle \geq 0 \qquad (14)$$

for all $r' = (r_1', \ldots, r_N') \in \mathcal{F}$, which is the first order optimality condition for solving Problem OC. It follows that $r^k \in \mathcal{O}$. On the other hand, if $r^k \in \mathcal{O}$, then $L(r^k) \leq L(r^{k+1}) \leq L(r^k)$. Hence,

$$L(r^{k+1}) = L(r^k) \Leftrightarrow r^{k+1} = r^k \Leftrightarrow r^k \in \mathcal{O}.$$

Finally, the facts that $\mathcal{F}$ is compact, every $r \in \mathcal{O}$ minimizes L, and $L(r^{k+1}) < L(r^k)$ if $r^k \notin \mathcal{O}$ imply that $r^k \to \mathcal{O}$ as $k \to \infty$. ■

Corollary 2: A charging profile r is stationary for Algorithm A1, i.e., if $r^{\bar{k}} = r$ for some $\bar{k} \geq 0$ then $r^k = r$ for all $k \geq \bar{k}$, if and only if $r \in \mathcal{O}$.

The proof of Corollary 2 follows from the fact that $r^{k+1} = r^k$ if and only if $r^k \in \mathcal{O}$ (shown in the proof for Theorem 3).

Theorem 4: Let r^* be an optimal charging profile. If $\mathcal{F}$ is non-empty, then

- the aggregated charging profile converges to that of r^*, i.e.,
$$\lim_{k \to \infty} R^k = R_{r^*};$$
- the price profile converges to that corresponding to r^*, i.e.,
$$\lim_{k \to \infty} p^k = U'(D + R_{r^*});$$
- for each EV n, the difference between two consecutive charging profiles vanishes, i.e.,
$$\lim_{k \to \infty} \left\| r_n^{k+1} - r_n^k \right\| = 0.$$

Proof: Theorem 3 implies that we can find a sequence $\{r^{*k}\}_{k \geq 1} \in \mathcal{O}$, such that $\|r^k - r^{*k}\| \to 0$ as $k \to \infty$. Since $\mathcal{O}$ is an equivalence class of $\sim$, $R_{r^{*k}} = R_{r^*}$. Hence $R^k \to R_{r^*}$ as $k \to \infty$. The price profile converges due to (9). Furthermore, the inequality in (13) implies that

$$L(r^k) - L(r^{k+1}) \geq \left(\frac{1}{\gamma} - N\beta \right) \sum_{n=1}^{N} \left\| r_n^{k+1} - r_n^k \right\|^2$$

for $k \geq 1$. Since $L(r^k) - L(r^{k+1}) \to 0$ as $k \to \infty$, it follows that for all $n \in \mathcal{N}$, $||r_n^{k+1} - r_n^k|| \to 0$ as $k \to \infty$. ■

Theorem 3 shows the convergence of r^k to the optimal set $\mathcal{O}$ while Theorem 4 focuses on the convergence of R^k and p^k to the optimal value R_{r^*} and $U'(D + R_{r^*})$. Since the change in the charging profile for EV n between consecutive iterations vanishes as $k \to \infty$, the objective function (8) approximates the "cost" after a certain number of iterations. It follows from (8) that

$$r_n^{k+1} = \underset{r_n \in \mathcal{F}_n}{\operatorname{argmin}} \left\| r_n - \left(r_n^k - \gamma \frac{\partial L}{\partial r_n} \right) \right\|^2$$

for $n \in \mathcal{N}$ and $k \geq 0$. Hence, Algorithm A1 is in fact a gradient projection method. Details on gradient projection methods can be found in, for example, [18, Chapter 3.3.2].

B. Asynchronous Decentralized Algorithm

The synchronous algorithm in section IV-A assumes that in each iteration, all EVs use the price profile in the last iteration to update their charging profiles, and the utility uses the new charging profiles to update the price. In reality, this synchronous computation may be impractical, especially when the number of EVs is large. In this section, we allow decisions to be made at different times with potentially outdated information. That is, in each iteration, only a subset of the EVs update their charging profiles, and the utility may or may not update the price. When an EV updates its charging profile, or the utility updates the price, they may use outdated information, i.e., information from the previous iterations.

We use an asynchronous model similar to that in [17], and allow EV $n \in \mathcal{N}$ to update at iterations $K_n \subseteq \{1, 2, \ldots\}$. At iterations $k \notin K_n$, we set $r_n^{k+1} = r_n^k$. Similarly let $K_u \subseteq \{1, 2, \ldots\}$ denote the set of iterations when the price is updated. At iterations $k \notin K_u$, we set $p^{k+1} = p^k$. At iterations $k \in K_n$, EV n updates its charging profile r_n^k according to (8), with p^k replaced by $p^{k - a_n(k)}$ due to delay $a_n(k)$. At iterations $k \in K_u$, the utility updates the price p^k according to (9), with r_n^k replaced by $r_n^{k - b_n(k)}$ due to delay $b_n(k)$. In general, we allow delays a_n and b_n to be k dependent but assume that they are uniformly bounded, i.e., $a_n(k) \leq d$, $b_n(k) \leq d$ for all n and all k. We also assume that each EV updates its charging profile at least once every d iterations, and the utility updates the price profile at least once every d iterations.

Algorithm A2:
Given planning horizon $\mathcal{T}$, the maximum number K of

iterations, error tolerance $\epsilon > 0$, base load profile D, the number N of EVs, charging rate sum R_n and charging rate upper bound $\overline{r}_n$ for EV $n \in \mathcal{N}$, pick a step size γ satisfying

$$0 < \gamma < \frac{1}{N\beta(3d+1)}.$$

1) Initialize the price profile and the charging profile as
$$p^0 := U'(D),\ r_n^0 := 0 \text{ for all } n.\ k \leftarrow 0.$$
2) If $k = 0$ or $k - 1 \in K_u$, the utility broadcasts γp^k to all EVs.
3) For each EV $n \in \mathcal{N}$, if $k \in K_n$, it calculates a new charging profile r_n^{k+1} as the solution to the following optimization problem
$$\begin{aligned} \min_{r_n} \quad & \sum_{t\in\mathcal{T}} \gamma p^{k-a_n}(t) r_n(t) + \frac{1}{2}\left(r_n(t) - r_n^k(t)\right)^2 \\ \text{s.t.} \quad & 0 \le r_n(t) \le \overline{r}_n(t),\ t \in \mathcal{T}; \\ & \sum_{t\in\mathcal{T}} r_n(t) = R_n, \end{aligned}$$
and reports r_n^{k+1} to the utility.
4) If $k \in K_u$, the utility updates the price profile p^{k+1} as
$$p^{k+1} := U'\left(D + \sum_{n=1}^{N} r_n^{k+1-b_n}\right).$$
If $\left\|p^{k+1} - p^k\right\| \le \epsilon$, return p^{k+1}, r_n^{k+1} for all n.
5) If $k < K$, $k \leftarrow k+1$, and go to step (2).
Else, return p^K, r_n^K for all n.

Similarly to the synchronous Algorithm A1 introduced in section IV-A, charging profile r^k of the asynchronous Algorithm A2 also converges to the set $\mathcal{O}$ as $k \to \infty$.

Theorem 5: If $\mathcal{F}$ is non-empty, then $r^k \to \mathcal{O}$ as $k \to \infty$. Let r^* be an optimal charging profile, then

- the aggregated charging profile converges to that of r^*, i.e., $\lim_{k\to\infty} R^k = R_{r^*}$;
- the price profile converges to that corresponding to r^*, i.e., $\lim_{k\to\infty} p^k = U'(D + R_{r^*})$;
- for each EV n, the difference between two consecutive charging profiles vanishes, i.e., $\lim_{k\to\infty} \left\|r_n^{k+1} - r_n^k\right\| = 0$.

Proof: The proof is given in the appendix. ■

Theorem 5 implies that even with outdated information and asynchronous updating of the charging profiles and prices, Algorithm A2 can still obtain optimal charging profiles, provided that the parameter γ is set properly. This optimality guarantee, again, is irrespective of the parameters $\overline{r}_n(t)$ and R_n. In other words, whatever the specifications of the EVs, whether they are homogeneous or not, Algorithm A2 always finds optimal charging profiles.

V. Case Studies

In this section, we first evaluate the optimality of Algorithm A1 and then compare the convergence rates of Algorithm A1 (synchronous) and Algorithm A2 (asynchronous). We compare the optimality and convergence rate of Algorithm A1 with those of the decentralized scheduling algorithm proposed in [13], in *homogeneous* and *non-homogeneous* cases. By *homogeneous*, we mean that all EVs have the same $\overline{r}_n$ and R_n (plug in for charging at the same time with the same deadline, and need to consume the same amount of energy at the same maximum charging rate). By *non-homogeneous*, we mean that $\overline{r}_n$ and R_n are not necessarily the same for the EVs (EVs may plug in at different times with different deadlines, and consume different amount of energy at different maximum charging rates). We do assume though all the EVs are available for negotiation at the beginning of the planning horizon. For notational brevity, we call the algorithm in [13] DAP, standing for "Deviation from Average Penalty." Recall that the optimality of DAP is only guaranteed in the homogeneous case.

We choose the average residential load profile in the service area of South California Edison from 20:00 on 02/13/2011 to 9:00 on 02/14//2011 as the average base demand profile per household. According to the typical charging characteristics of EVs in [15], we set $r_n^{max} = 3.3$kW. We assume that the charging rate $r_n(t)$ of EV n at slot t can take continuous values in $[0, r_n^{max}]$ after EV n plugs in for charging and before its deadline. We consider the penetration level of $N = 20$ EVs in 100 households. The planning horizon is from 20:00 to 9:00 the next day, and divided into 52 slots of 15 minutes, during which the charging rate of an EV is a constant. The map $U : \mathbb{R} \to \mathbb{R}$ is taken to be $U(x) = \frac{1}{2}x^2$. As used in [13], we choose the price function and parameters for Algorithm DAP as $p(x) = 0.15x^2$, $c = 1$, and $\delta = 0.15$.

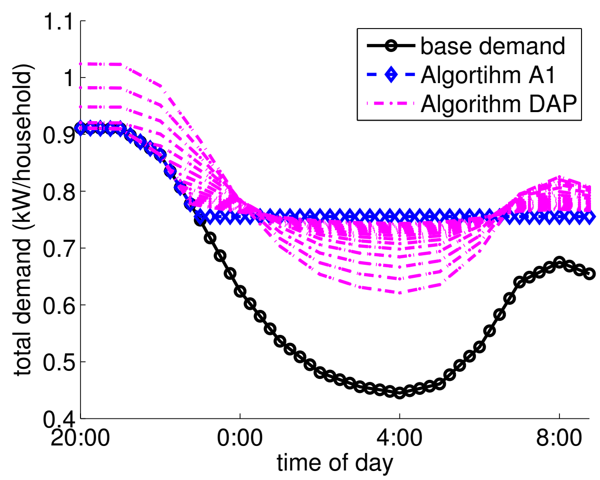

Fig. 4. All EVs plug in at 20:00 with deadline at 9:00 on the next day, and have 10kWh charging capacity. Multiple purple dash-dot curves correspond to total demand in different iterations of Algorithm DAP.

Homogeneous case: Algorithm A1 obtains optimal charging profiles, whatever the parameters $\overline{r}_n(t)$ and R_n are. Even if the EVs are non-homogeneous, with arbitrary plug-in times, deadlines, charging capacities, and maximum charging rates, Algorithm A1 still obtains optimal charging profiles. We choose to simulate the homogeneous case only to compare Algorithm A1 with Algorithm DAP, since Algorithm DAP is optimal only when the EVs are homogeneous. In this example, all the EVs have the same deadline at 9:00 the next morning. Figure 4 shows the average total demand profile in each

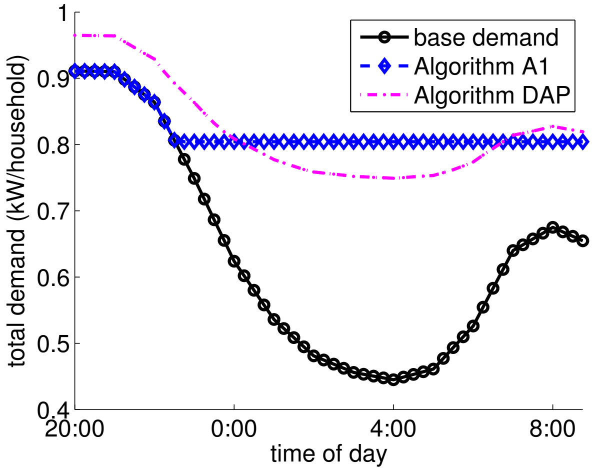

Fig. 5. All EVs plug in at 20:00 with deadline at 9:00 on the next day, but have different charging capacities uniformly distributed in $[0, 20]$kWh.

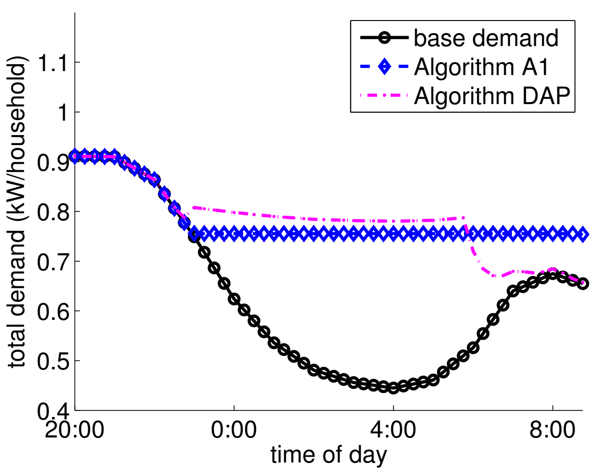

Fig. 6. All EVs have 10kWh charging capacity, but plug in at different times (uniformly between 20:00 and 23:00) with different deadlines (uniformly distributed from 6:00 to 9:00 on the next day).

iteration of Algorithm A1 and DAP in a homogeneous case. Both algorithms converge to a flat charging profile. Moreover, Algorithm A1 converges with a single iteration, while DAP takes several iterations to converge.

Non-homogeneous capacities: Figure 5 shows the average total demand profiles at convergence of Algorithms A1 and DAP in a non-homogeneous case where EVs have different charging capacities. Algorithm A1 still converges to a flat charging profile in a few iterations while DAP no longer converges to a flat charging profile. The optimality proof provided in [13] does not straightforwardly extend to non-homogeneous cases. Algorithm A1 is proved to achieve optimal charging profiles, whatever the parameters $\overline{r}_n(t)$ and R_n are ($\overline{r}_n(t)$ takes care of the plug in time and deadline of the EVs, as well as its maximum charging rate r_n^{max}). We show another source of non-homogeneous, under which the difference between Algorithm A1 and DAP is more significant.

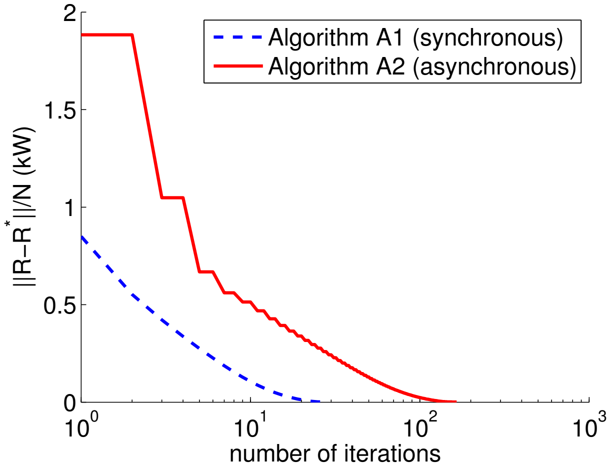

Fig. 7. The l_2 norm $\frac{1}{N}\|R^k - R^*\|$ of the normalized difference $\frac{1}{N}(R^k - R^*)$ between the aggregated charging profile R^k in iteration k in Algorithms A1 or A2 and the optimal aggregated charging profile. EVs (all with 10kWh charging capacity) plug in uniformly between 20:00 and 23:00 with deadlines uniformly distributed from 6:00 to 9:00 on the next day. In the asynchronous setting, all EVs update their charging profiles and the utility updates price profile in iteration $k = 1, 3, 5, \ldots$, with outdated information $\hat{p}^{k-1} = p^{k-2}$ and $\hat{r}_n^k = r_n^{k-1}$.

Non-homogeneous plug-in times and deadlines: Figure 6 shows the average total demand profiles in another non-homogeneous case where EVs have the same charging capacity, but different plug-in times and deadlines. Note that, in this example, an optimal charging profile is not flat, since most of the EVs have a deadline earlier than 9:00, leading to significantly lower total demand near 9:00. Algorithm A1 still converges to an optimal charging profile within few iterations, while Algorithm DAP yields a charging profile far from optimal. This is because Algorithm DAP uses a penalty term to limit the deviation of the EV charging profiles from the average charging profile. EVs have different charging horizons, but have to track the same average charging profile. At higher EV penetration levels, the difference becomes more significant. Algorithm A1 changes “deviation from the average penalty” to “deviation from the last iteration penalty”. While preserving its convergence property, Algorithm A1 no longer requires different EVs to track a common average charging profile. Hence, it successfully deals with the issue of heterogeneity in charging deadlines. In fact, Theorem 3 and 4 tell us that Algorithm A1 is always optimal, even if the EVs are completely non-homogeneous. They may plug in for charging at different times with different deadlines, and consume different amount of energy at different maximum charging rates, but Algorithm A1 always achieves optimal total demand profile.

Comparison of convergence rates of synchronous and asynchronous algorithms: According to Theorem 5, Algorithm A2 obtains optimal charging profiles at convergence, just as Algorithm A1. This result is validated by the same set of simulations we did for Algorithm A1. We do not show the steady-state total demand profiles for Algorithm A2 in these simulations since they are the same as those of Algorithm A1

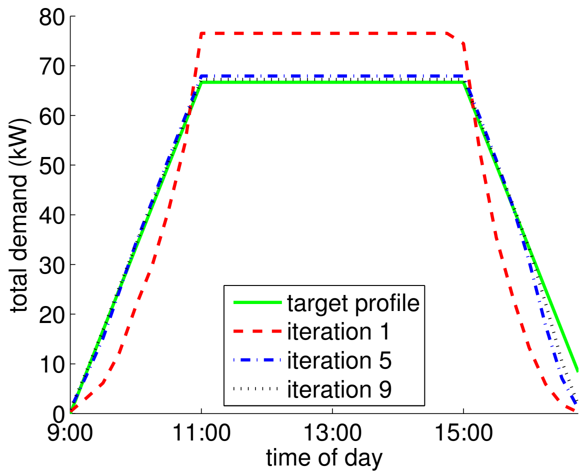

Fig. 8. 40 EVs plug in uniformly between 9:00 and 11:00 with deadlines uniformly distributed from 15:00 to 17:00. All the EVs need to charge 10kWh of energy. The target profile is shown by the green curve, and aggregate demand profiles in iteration 1, 5, 9 of Algorithm A1 are shown by the red dash, blue dash-dot, and black dot curves, respectively.

in Figure 4, 5 and 6. Instead, we compare the convergence rate of Algorithm A1 and A2 in Figure 7. It can be seen that the asynchronous Algorithm A2 takes more iterations to converge to optimal charging profiles, which is not surprising, since an EV does not necessarily update its charging profile in each iteration, and when it does, it may use outdated information. However, Algorithm A2 still converges if delay is bounded and γ is chosen properly. This makes Algorithm A2 robust to communication delays and failures.

VI. Extensions

A. Tracking a Given Profile

As it is known, the energy for EV charging might be provided by a utility or a load aggregator. For the utility, the objective is to control EV charging in order to flatten the load profile, and this is discussed in the previous sections. A load aggregator that sells energy to EVs will have to buy energy in the electricity market in a day-ahead basis. So, in the day after market negotiations, the objective of a load aggregator will be minimizing the deviations between energy G bought in the day-ahead market and the energy effectively consumed by the EVs, instead of flattening the load profile.

The algorithms proposed in this paper can be extended to the objective of tracking a target load profile G pre-specified by the load aggregator, which is captured by minimizing

$$J(r) = J(r_1, \ldots, r_N) := \sum_{t=1}^{T} \left(\sum_{n=1}^{N} r_n(t) - G(t) \right)^2. \quad (15)$$

Note that equation (15) is equivalent to equation (1) with $U(x) = x^2$ and $D(t) = -G(t)$.

Figure 8 shows a simulation result of tracking a given target profile. An aggregator charges the batteries of 40 EVs, which plug in at times uniformly distributed from 9:00 to 11:00, with deadlines uniformly distributed from 15:00 to 17:00. All the EVs specify 10kWh charging capacity. The target profile G is shown by the black curve, and the blue dash-dot curves correspond to the aggregated charging profiles R in iteration 1, 5, 9 of Algorithm A1. It can be seen that R is almost the same as G after 9 iterations. The small difference between R and G comes from early deadlines of the EVs in this example.

B. Online Algorithm

The algorithms proposed in this paper are offline in the sense that all EVs are available for negotiation at the beginning of the planning horizon, and decisions are made with full information about each EV. A more realistic model, that we call online, would incorporate the EVs as they become available for negotiation, e.g., when they plug in for charging, over time. Moreover, since the state of the system changes over time, the problem data would be updated over time. Our preliminary work has focused on modifications of Algorithm A1 in an online setup.

We call EV n active at time slot t if it is available for negotiation at t and needs to be charged $R_n^t \Delta T > 0$ amount of energy by deadline $d_n \geq t$. Let N_t denote the number of active EVs at slot t. An online algorithm requires participation of only active EVs $n \in \mathcal{N}_t$ at slot t. In algorithm A1, it is assumed that all the EVs are available for negotiation at slot $t = 0$. Now we consider the case where EVs become available for negotiation over time, i.e., some EVs become available for negotiation at slot 1, some at slot 2, etc. The online algorithm works as follows.

Online A1:
Given the number K of iterations in each time slot, base demand D known to the utility. Pick a step size γ satisfying $0 < \gamma < \frac{1}{\beta}$, and horizon T that will cover the deadlines of all active EVs. At slot $t = 0, 1, \ldots$, repeat the following steps:

1) **Initialization:** $k \leftarrow 0$. For all active EVs $n \in \mathcal{N}_t$,
$$r_n^k = \begin{cases} 0 & \text{if } n \text{ is new to negotiate} \\ r_n^K & \text{if } n \text{ negotiated in slot } t-1, \end{cases}$$
where r_n^K refers to the negotiation result in slot $t-1$.
2) **Iteration k:** The utility knows r_n^k, and computes and broadcasts price signal
$$p^k(\tau) := \frac{1}{N_t} U' \left(D(\tau) + \sum_{n=1}^{N_t} r_n^k(\tau) \right)$$
for $t \leq \tau \leq t + T$ to all the active EVs $n \in \mathcal{N}_t$.
3) Each EV $n \in \mathcal{N}_t$ knows the charging capacity R_n^t at slot t (amount of energy to be charged from t on), its deadline d_n, and charging rate upper bound $\overline{r}_n$. It calculates a new charging profile r_n^{k+1} as the solution to the following optimization problem
$$\begin{aligned} \underset{r_n}{\text{minimize}} \quad & \sum_{\tau=t}^{d_n} p^k(\tau) r_n(\tau) + \frac{1}{2\gamma} \left(r_n(\tau) - r_n^k(\tau) \right)^2 \\ \text{subject to} \quad & 0 \leq r_n(\tau) \leq \overline{r}_n(\tau), \ t \leq \tau \leq d_n \\ & \sum_{\tau=t}^{d_n} r_n(\tau) = R_n^t. \end{aligned}$$
The EV reports r_n^{k+1} to the utility.

4) $k \leftarrow k+1$. If $k < K$, go to step 2).
5) **Set** $t \leftarrow t+1$**:** EV $n \in N_t$ charges at rate $r_n^K(t)$ during slot t, and update R_n^t to $R_n^{t+1} = R_n^t - r_n^K(t)$. If $R_n^{t+1} = 0$ or $d_n < t+1$, EV n becomes inactive. If an EV comes for charging or negotiation, it becomes active. The utility keeps track of the new number N_{t+1} of active EVs at slot $t+1$. Go to step 1).

It can be seen that Algorithm Online A1 roughly implements Algorithm A1 at each time slot. Though theoretical investigation of Online A1 is subject to current research, simulations shown in Figure 9-12 suggest that Online A1 has good performance, even in the presence uncertain EV arrivals.

In Figure 9-12, 20 EVs (out of 100 households) participate negotiating on their charging profiles when they plug in for charging, with the same deadline at 9:00 the next morning, and 10kWh charging capacity. From Figure 9 to Figure 12, EVs arrival with increasing uncertainty. It can be seen that as arrival uncertainty increases, total demand profile (red dash-dot curve) obtained by Online A1 deviates more from the optimal (blue dash curve). The peak demand (after 0:00) remains close to that of the optimal profile, until the EV arrival uncertainty becomes very large — EVs can plug in till 5:00.

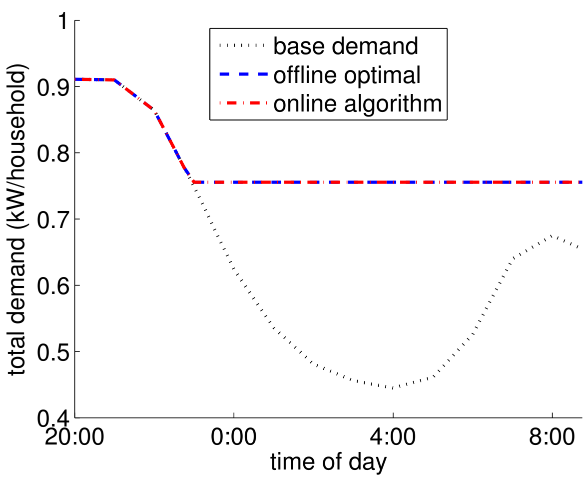

Fig. 9. EVs plug in uniformly between 20:00 and 23:00.

VII. Conclusions

In this paper, we studied utilizing decentralized EV charging control to fill the overnight electricity demand valley. We formulated it as an optimization problem, and showed that optimal charging profile minimizes the l_2 norm of the total demand. We proposed decentralized offline and online algorithms for solving the problem. In each iteration of these algorithms, each EV calculates its own charging profile according to the price profile broadcast by the utility, and the utility guides their behavior by updating the price profile. We proved that the offline algorithms converge to optimal charging profiles, and showed that online algorithms yield nearly flat charging profiles, with only a scalar prediction of future EV charging demand. Simulation results are used to illustrate and validate these results.

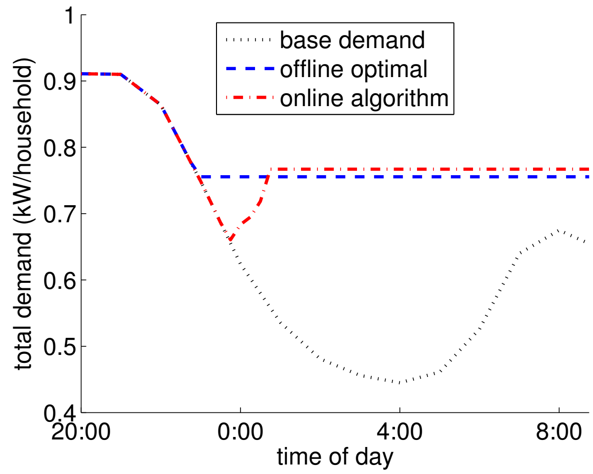

Fig. 10. EVs plug in uniformly between 20:00 and 1:00.

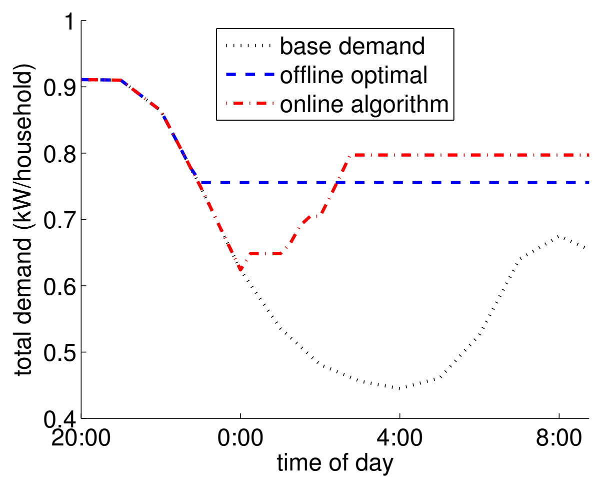

Fig. 11. EVs plug in uniformly between 20:00 and 3:00.

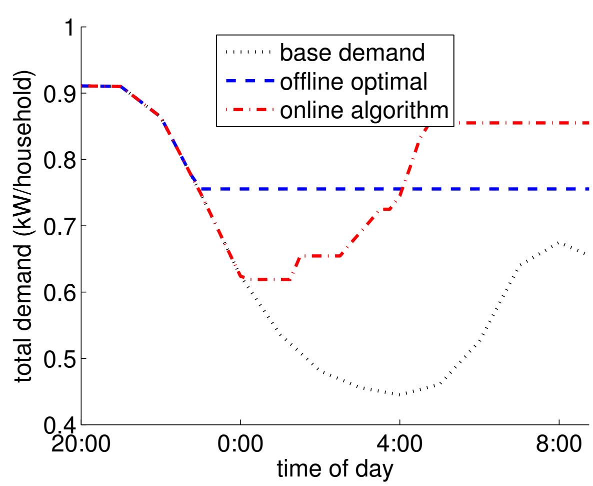

Fig. 12. EVs plug in uniformly between 20:00 and 5:00.

APPENDIX

Lemma 3: Define $\pi_k := \sum_{n=1}^{N} \left\|r_n^{k+1} - r_n^k\right\|$. If $\mathcal{F}$ is non-empty and $\gamma < \frac{1}{N\beta(3d+1)}$, then $\pi_k \to 0$ as $k \to \infty$.

Proof: If $\mathcal{F}$ is non-empty, $\mathcal{F}_n$ is non-empty for all $n \in \mathcal{N}$. By repeating the proof in Lemma 1, we can show that

$$\left\langle p^{k-a_n}, r_n^{k+1} - r_n^k \right\rangle \le -\frac{1}{\gamma}\left\|r_n^{k+1} - r_n^k\right\|_2^2$$

for $n \in \mathcal{N}$ and $k \ge 1$. Hence,

$$\begin{aligned}
&\left\langle U'\left(D^{k+1}\right), r_n^{k+1} - r_n^k \right\rangle \\
&= \left\langle p^{k-a_n}, r_n^{k+1} - r_n^k \right\rangle + \left\langle U'\left(D^{k+1}\right) - p^{k-a_n}, r_n^{k+1} - r_n^k \right\rangle \\
&\le -\tfrac{1}{\gamma}\left\|r_n^{k+1} - r_n^k\right\|^2 + \left\|U'\left(D^{k+1}\right) - p^{k-a_n}\right\| \left\|r_n^{k+1} - r_n^k\right\|
\end{aligned}$$

for $n \in \mathcal{N}$ and $k \ge 1$. Choose $c \ge 0$ such that

$$k - a_n - c = \min\{l \le k - a_n \mid l - 1 \in K_u\}.$$

Then, $0 \le c \le d-1$ and

$$\begin{aligned}
&\left\langle U'\left(D^{k+1}\right), r_n^{k+1} - r_n^k \right\rangle + \tfrac{1}{\gamma}\left\|r_n^{k+1} - r_n^k\right\|^2 \\
&\le \left\|r_n^{k+1} - r_n^k\right\| \left\|U'\left(D^{k+1}\right) - p^{k-a_n-c}\right\| \\
&= \left\|r_n^{k+1} - r_n^k\right\| \\
&\qquad \cdot \left\|U'\left(D^{k+1}\right) - U'\left(D + \textstyle\sum_{n=1}^{N} r_n^{k-a_n-c-b_n}\right)\right\| \\
&\le \beta\left\|r_n^{k+1} - r_n^k\right\| \left\|R^{k+1} - \textstyle\sum_{n=1}^{N} r_n^{k-a_n-c-b_n}\right\| \\
&\le \beta\left\|r_n^{k+1} - r_n^k\right\| \left(\textstyle\sum_{n=1}^{N} \left\|r_n^{k+1} - r_n^{k-a_n-c-b_n}\right\|\right) \\
&\le \beta\left\|r_n^{k+1} - r_n^k\right\| \left(\textstyle\sum_{n=1}^{N}\sum_{l=k-a_n-c-b_n}^{k} \left\|r_n^{l+1} - r_n^l\right\|\right) \\
&\le \beta\left\|r_n^{k+1} - r_n^k\right\| \left(\textstyle\sum_{n=1}^{N}\sum_{l=k-3d}^{k} \left\|r_n^{l+1} - r_n^l\right\|\right)
\end{aligned}$$

for $n \in \mathcal{N}$ and $k \ge 1$. Then,

$$\begin{aligned}
&\left\langle U'\left(D^{k+1}\right), R^{k+1} - R^k \right\rangle + \frac{1}{\gamma}\sum_{n=1}^{N}\left\|r_n^{k+1} - r_n^k\right\|^2 \\
\le\ & \beta \sum_{m=1}^{N} \left\|r_m^{k+1} - r_m^k\right\| \sum_{n=1}^{N}\sum_{l=k-3d}^{k} \left\|r_n^{l+1} - r_n^l\right\| \\
=\ & \beta\pi_k \sum_{l=k-3d}^{k} \pi_l \\
\le\ & \beta\left(\left(1 + \frac{3d}{2}\right)\pi_k^2 + \frac{1}{2}\sum_{l=k-3d}^{k-1} \pi_l^2\right)
\end{aligned}$$

for $k \ge 1$. Hence,

$$\begin{aligned}
& L(r^{k+1}) - L(r^k) \\
\le\ & \left\langle U'\left(D^{k+1}\right), R^{k+1} - R^k \right\rangle \\
\le\ & \beta\left(\left(1 + \frac{3d}{2}\right)\pi_k^2 + \frac{1}{2}\sum_{l=k-3d}^{k-1} \pi_l^2\right) \\
& \qquad - \frac{1}{\gamma}\sum_{n=1}^{N}\left\|r_n^{k+1} - r_n^k\right\|^2 \\
\le\ & \frac{\beta}{2}\sum_{l=k-3d}^{k-1} \pi_l^2 + \left(\beta\left(1 + \frac{3d}{2}\right) - \frac{1}{N\gamma}\right)\pi_k^2
\end{aligned}$$

for $k \ge 1$ and

$$\begin{aligned}
& L(r^{k+1}) - L(r^1) \\
\le\ & \frac{3d}{2}\beta\sum_{l=0}^{k-1} \pi_l^2 + \left(\beta\left(1 + \frac{3d}{2}\right) - \frac{1}{N\gamma}\right)\sum_{l=1}^{k} \pi_l^2 \\
\le\ & \left(\beta(3d+1) - \frac{1}{N\gamma}\right)\sum_{l=1}^{k} \pi_l^2 + \frac{3d}{2}\beta\pi_0^2. \qquad (16)
\end{aligned}$$

Since $\gamma < \frac{1}{N\beta(3d+1)}$,

$$\beta(3d+1) - \frac{1}{N\gamma} < 0. \qquad (17)$$

If π_k does not converge to 0 as k tends to infinity, then $L(r^{k+1}) \to -\infty$ as $k \to \infty$. However, $L(r^{k+1})$ is bounded below by its definition. Hence, $\pi_k \to 0$ as $k \to \infty$. ■

As a consequence of Lemma 3,

$$\begin{aligned}
& \left\|U'(D^{k+1}) - U'(D^k)\right\| \\
\le\ & \beta\|R^{k+1} - R^k\| \\
\le\ & \beta\pi_k \to 0 \text{ as } k \to \infty.
\end{aligned}$$

Similarly, $\left\|p^k - U'(D^k)\right\| \to 0$ as $k \to \infty$. This implies that, after a number of iterations, real price profile $U'(D^k)$ and its delayed version p^k (used by EVs to update their charging profiles) become close, and we can expect that our algorithm converges to optimal charging profiles even with delay.

For a given charging profile r, define the distance to the set of optimal charging profiles as following

$$d(r, \mathcal{O}) := \inf_{r' \in \mathcal{O}} \|r - r'\|.$$

Lemma 4: For a sequence $\left\{r^k\right\}_{k\ge 1} \subseteq \mathcal{F}$ of feasible charging profiles, if $d(r^k, \mathcal{O})$ does not converge to 0 as $k \to \infty$, then there exist a positive constant $\delta > 0$ and a subsequence $\left\{r^{k_i}\right\}_{i\ge 1}$ such that

$$k_{i+1} - k_i \ge d, \qquad (18)$$

$$d(r^{k_i}, \mathcal{O}) \ge \delta. \qquad (19)$$

for $i \ge 1$.

Proof: If $d(r^k, \mathcal{O})$ does not converge to 0 as $k \to \infty$, then there exists $\delta > 0$, such that for any $K \in \mathbb{N}$, there exists $k > K$ with

$$d(r^k, \mathcal{O}) \ge \delta.$$

We construct the subsequence $\left\{r^{k_i}\right\}_{i\ge 1}$ as following:

- Let $K = 1$, choose $k_1 > K$ such that $d(r^{k_1}, \mathcal{O}) \ge \delta$.
- Suppose we already get $k_1, \ldots, k_m$ ($m \ge 1$), satisfying (18) for $i = 1, \ldots, m-1$ and (19) for $i = 1, \ldots, m$. Let $K = k_m + d$, choose $k_{m+1} > K$ such that $d(r^{k_{m+1}}, \mathcal{O}) \ge \delta$.

It is easy to check that the subsequence $\left\{r^{k_i}\right\}_{i\ge 1}$ satisfies (18) and (19) for $i \ge 1$ by induction. ■

Proof for Theorem 5: Denote r^k as the charging profile of all EVs in iteration k of Algorithm A2. We first prove that $r^k \to \mathcal{O}$ as $k \to \infty$ by contradiction. Assume that r^k does not converge to the set $\mathcal{O}$ as $k \to \infty$, then $d(r^k, \mathcal{O})$ does not converge to 0. By Lemma 4, we can find a subsequence

$\{r^{k_i}\}_{i\geq 1}$ satisfying (18) and (19) for $i \geq 1$. Since $\mathcal{F}$ is compact, we can find a convergent subsequence $\{r^{k_{i_s}}\}_{s\geq 1}$ of $\{r^{k_i}\}_{i\geq 1}$ such that

$$r^{k_{i_s}} \to r^* = (r_1^*, \ldots, r_N^*) \text{ as } s \to \infty.$$

It's not difficult to show that $d(r^*, \mathcal{O}) \geq \delta$. For brevity, we use $\{r^{k_i}\}_{i\geq 1}$ to denote the sequence $\{r^{k_{i_s}}\}_{s\geq 1}$, then

$$r^{k_i} \to r^* = (r_1^*, \ldots, r_N^*) \text{ as } i \to \infty.$$

Lemma 3 implies that $\pi_k \to 0$ as $k \to \infty$. Hence, $r^{k_i+j} \to r^*$ as $i \to \infty$ for all $j \in \{0, \ldots, d-1\}$. Define

$$p^* := U'(D + R_{r^*}).$$

Since $r^* \notin \mathcal{O}$, r^* is not a stationary point for Algorithm A1 (Corollary 2). Hence, there exists n such that

$$r_n' := \operatorname*{argmin}_{r_n \in \mathcal{F}_n} \langle p^*, r_n \rangle + \frac{1}{2\gamma}\|r_n - r_n^*\|^2 \neq r_n^*.$$

EV n updates its charging profile r_n at least once during iterations $[k_i, k_i + d - 1]$ for $i \geq 1$. Assume that it updates at iteration $k_i + j_i$ where $j_i \in [0, d-1]$, then

$$\|r_n^{k_i+j_i+1} - r_n^{k_i+j_i}\| \to \|r_n' - r_n^*\| > 0 \text{ as } i \to \infty.$$

Hence, for i sufficiently large,

$$\sum_{l=k_i}^{k_i+d-1} \pi_l \geq \pi_{k_i+j_i} \geq \|r_n^{k_i+j_i+1} - r_n^{k_i+j_i}\| > \frac{1}{2}\|r_n' - r_n^*\| > 0$$

and

$$\sum_{l=k_i}^{k_i+d-1} \pi_l^2 \geq \frac{1}{d}\left(\sum_{l=k_i}^{k_i+d-1} \pi_l\right)^2 > \frac{1}{4d}\|r_n' - r_n^*\|^2 > 0.$$

It follows from (16) that $L(r^{k+1}) \to -\infty$ as $k \to \infty$. However, $L(r^{k+1})$ is bounded below by its definition, contradict. Hence, $r^k \to \mathcal{O}$ as $k \to \infty$. The rest of the proof follows along the lines of that for Theorem 4.

Acknowledgment

The authors express gratitude to K. Mani Chandy and Sachin Adlakha for inspiring discussions. We would also like to thank ARO grant W911NF-08-1-0233, Bell Labs of Lucent-Alcatel, NSF NetSE grants CNS 0911041, Southern California Edison (SCE), Okawa Foundation, Boeing Corporation and Cisco.

References

[1] "Environmental assessment of plug-in hybrid electric vehicles - volume 1: nationwide greenhouse gas Emissions," Electric Power Research Institute, 2007. Available: http://my.epri.com/portal/server.pt?

[2] Committee on assessment of resource needs for full cell and hydrogen technologies, National Research Council, *Transitions to alternative transportation technologies–plug-in hybrid electric vehicles*, the National Press, 2010.

[3] U.S. Department of Energy website http://www.eere.energy.gov/. Available: http://tinyurl.com/4o5ggml

[4] L. Kelly, A. Rowe and P. Wild, "Analyzing the impacts of plug-in electric vehicles on distribution networks in British Columbia," *in Proc. Electrical Power & Energy Conference*, 2009, pp. 1-6.

[5] C. Roe, F. Evangelos, J. Meisel, A. P. Meliopoulos and T. Overbye, "Power system level impacts of PHEVs," *in Proc. Hawaii International Conference on System Science*, 2009, pp. 1-10.

[6] K. Clement, E. Haesen and J. Driesen, "Coordinated charging of multiple plug-in hybrid electric vehicles in residential distribution grids," *in Proc. Power Systems Conference and Exposition*, 2009, pp. 1-7.

[7] J. A. P. Lopes, F. J. Soares and P. M. R. Almeida, "Integration of electric vehicles in the clectric power system," *Proceedings of the IEEE*, vol. 99, No. 1, 2011, pp. 168-183.

[8] C. Quinn, D. Zimmerle and T. H. Bradley, "The effect of communication architecture on the availability, reliability, and economics of plug-in hybrid electric vehicle-to-grid ancillary services," *Journal of Power Sources*, vol. 195, issue 5, 2010, pp. 1500-1509.

[9] J. A. P. Lopes, P. M. R. Almeida, and A. M. M. da Silva, "Smart charging strategies for electric vehicles: Enhancing grid performance and maximizing the use of variable renewable energy sources," *in Proc. International Battery, Hybrid and Fuel Cell Electric Vehicle Symposium and Exhibition*, 2009, pp. 1-11.

[10] S. Shao, T. Zhang, M. Pipattanasomporn and S. Rahman, "Impact of TOU rates on distribution load shapes in a smart grid with PHEV penetration," *in Proc. Transmission and Distribution Conference and Exposition*, 2010, pp. 1-6.

[11] E. Sortomme, M. M. Hindi, S. D. J. MacPherson and S. S. Venkata, "Coordinated charging of plug-in hybrid electric vehicles to minimize distribution system losses," *IEEE Transactions on Smart Grid*, vol. 2, no. 1, 2011, pp. 198-205.

[12] M. C. Caramanis and J. M. Foster, "Coupling of day ahead and real-time power markets for energy and reserves incorporating local distribution network costs and congestion," *in Proc. Allerton Conference on Communication, Control, and Computing*, 2010, pp. 42-49.

[13] Z. Ma, D. Callaway and I. Hiskens, "Decentralized charging control for large populations of plug-in vehicles," *in Proc. Conference on Decision and Control*, 2010, pp. 206-212.

[14] A. Ipakchi and F. Albuyeh, "Grid of the future," *IEEE Power and Energy Magazine*, vol. 7, no. 2, 2009, pp. 52-62.

[15] South California Edison website http://www.sce.com/. Available: http://www.sce.com/005_regul_info/eca/DOMSM11.DLP

[16] S. H. Low and D. E. Lapsley, "Optimization flow control, I: Basic algorithm and convergence," *IEEE/ACM Transactions on Networking*, 1999, pp. 861-874.

[17] D. P. Bertsekas and J. N. Tsitsiklis, "Parallel and Distributed Computation," Prentice-Hall, 1989.

[18] S. Boyd and L. Vandenberghe, "Convex Optimization," Cambridge University Press, 2004.